ELSEVIER

Journal of Magnetism and Magnetic Materials 169 (1997) 323–334

journal of magnetism and magnetic materials

Intra-potential-well contribution to the AC susceptibility of a noninteracting nano-sized magnetic particle system

P. Svedlindh[a,*], T. Jonsson[a], J.L. García-Palacios[b]

[a] *Department of Technology, Uppsala University, Box 534, S-751 21 Uppsala, Sweden*
[b] *Instituto de Ciencia de Materiales de Araógn, Universidad de Zaragoza-CSIC, 50015 Zaragoza, Spain*

Received 11 October 1996; revised 11 December 1996

Abstract

The model proposed by Shliomis and Stepanov (J. Magn. Magn. Mater. 122 (1993) 176) to describe the low field magnetic response of a solid dispersion of noninteracting nano-sized particles has been used to calculate the temperature dependence of the AC susceptibility of a particle system with a known particle size distribution. A comparison with experimental AC susceptibility results shows the necessity of including both an inter-potential- and an intra-potential-well contribution to the magnetic response. Moreover, different relaxation times need to be assigned to the two contributions.

PACS: 75.50.Mm; 75.70.Tt

Keywords: Ferrofluid; Small magnetic particles; AC susceptibility; Magnetic response

1. Introduction

The magnetic response of single-domain magnetic particles has been in focus since the pioneering work of Néel [1]. In a noninteracting particle ensemble, with uniaxial magnetic anisotropy and the easy axes of the magnetic particles distributed at random, it was found that the low field equilibrium susceptibility does not depend on the magnetic anisotropy of the particles [2]. Hence, the susceptibility corresponds to that derived in a simple superparamagnetic model where the anisotropy is neglected. The main effect of the magnetic anisotropy is to introduce energy barriers that the particle magnetic moments need to overcome before equilibrium is reached, implying that the particle ensemble could, depending on the experimental observation time, display magnetic relaxation. The relaxation mechanism corresponds to an orientational redistribution of the particle magnetic moments according to conditions set by the magnetic anisotropy, applied magnetic field and temperature. The relaxation can be envisaged as a two-stage process: firstly, the magnetic moments redistribute inside the potential wells with a relaxation time of the order of the inverse of the

* Corresponding author. Tel.: + 46 18 18 2500; fax: + 46 18 15 5095.

PII S0304-8853(96)00756-1

precession frequency of the magnetic moments in the anisotropy field ($\sim 10^{-9}$–10^{-12} s); secondly, the equilibration between the potential wells, which is a thermally activated process, proceeds. This latter mechanism can result in exceedingly slow magnetic after effects since its characteristic time, which essentially follows the Néel–Brown theory [1, 3], ranges from picoseconds to geological time scales depending on the anisotropy energy barrier, temperature, and applied magnetic field.

Recently, several experimental methods using results obtained from AC susceptibility [4, 5] and magnetic relaxation measurements [4, 6–8] have been developed to extract information about the distribution of energy barriers in nano-sized magnetic particle systems. The developed methods make certain assumptions concerning the equilibrium magnetic response and the relaxation mechanisms responsible for the observed frequency or time-dependent properties of the magnetic particle system. Consistency of the methods requires that the extracted energy barrier distribution, when inserted in the model used to obtain the barrier distribution, should be able to reproduce the experimental results. For instance, using the out-of-phase component of the AC susceptibility to determine the distribution of energy barriers [4], consistency requires that the extracted distribution should be able to reproduce both the in-phase and out-of-phase components of the AC susceptibility. Having proved consistency, it is also possible to assert that the model employed is a reliable model.

In this paper we present AC susceptibility results of a frozen ferrofluid having the easy axes of the magnetic single-domain particles oriented at random. The experimental results are modelled using the previously determined [4] energy barrier distribution. It is shown that in order to be able to model both the in-phase and out-of-phase components of the AC susceptibility, inter-potential as well as intra-potential-well contributions to the magnetic response have to be included in the theoretical model. Moreover, different relaxation times have to be assigned to the two responses.

The structure of this paper is as follows: in Section 2 some experimental details are described; in Section 3 expressions for the low field magnetic response of a solid dispersion of noninteracting small magnetic particles are reviewed. Consequences for experimental methods using AC susceptibility results to determine the particle size distribution are also pointed out. In Section 5 these expressions are used to model the experimental data. The necessity of including an intra-potential-well contribution to the magnetic response of the nano-sized particle system is also discussed.

2. Experimental

The experiments were done on a sample consisting of nano-sized maghemite, γ-Fe_2O_3, particles [9]. The particles, having a median particle diameter of 8 nm, were suspended in hydrocarbon oil and coated with a surfactant layer to prevent the particles from agglomerating. Since the measurements were made at low temperatures, the oil was frozen and the particles fixed randomly in the sample. At low temperatures the saturation magnetisation of maghemite is $M_s = 420$ kA/m [10]. The concentration by volume of particles was $\sim 0.03\%$, which is low enough to safely rule out any influence of dipole–dipole interactions on the measured magnetic dynamics [11].

The AC susceptibility measurements were performed in a LakeShore 7225 AC susceptometer, using a sample cup containing 0.15 ml of the particle suspension. To avoid nonlinear magnetisation effects the field used was 0.1 mT.

3. Theoretical background

3.1. Linear susceptibility of independent particles

We will restrict our attention to a solid dispersion of noninteracting single domain magnetic particles with uniaxial magnetic anisotropy. The expression for the equilibrium initial susceptibility of such a system has been independently derived by several authors [2]. Nevertheless, we will in the following present a slightly different derivation, leading to the same equation for the equilibrium initial susceptibility as derived by others. Finally, we will discuss the formula proposed by Shliomis and Stepanov [12] for the dynamic susceptibility.

The total magnetic potential for a particle of volume V in the external field $\boldsymbol{H}$ is given by

$$E = -KV(\boldsymbol{e}\cdot\boldsymbol{n})^2 - \mu_0 M_s V H(\boldsymbol{e}\cdot\boldsymbol{h}), \tag{1}$$

where K is the uniaxial-anisotropy energy constant and, $\boldsymbol{n}$, $\boldsymbol{h}$ and $\boldsymbol{e}$ are unit vectors along the anisotropy axis, applied field and particle magnetic moment, respectively.

The linear equilibrium susceptibility is related to the fluctuations of the magnetic moment by

$$\chi = \mu_0 M_s^2 V \frac{\langle(\boldsymbol{e}\cdot\boldsymbol{h})^2\rangle_0 - \langle\boldsymbol{e}\cdot\boldsymbol{h}\rangle_0^2}{k_B T}. \tag{2}$$

The zero subscript in the above equation denotes that the thermal average is taken in the zero field limit, e.g.

$$\langle(\boldsymbol{e}\cdot\boldsymbol{h})^2\rangle_0 = \frac{\int \mathrm{d}\Omega\,(\boldsymbol{e}\cdot\boldsymbol{h})^2 \exp[\sigma(\boldsymbol{e}\cdot\boldsymbol{n})^2]}{\int \mathrm{d}\Omega \exp[\sigma(\boldsymbol{e}\cdot\boldsymbol{n})^2]}, \tag{3}$$

where $\sigma = KV/k_B T$ and $\mathrm{d}\Omega = \mathrm{d}\phi\,\mathrm{d}\theta\sin(\theta)$, with (θ,ϕ) denoting the angular coordinates of $\boldsymbol{e}$. Note that $\langle\boldsymbol{e}\cdot\boldsymbol{h}\rangle_0 = 0$ since $(\boldsymbol{e}\cdot\boldsymbol{h})$ reverses its sign when $\boldsymbol{e}\to-\boldsymbol{e}$. It is thus enough to calculate $\langle(\boldsymbol{e}\cdot\boldsymbol{h})^2\rangle_0$ to obtain χ. With $\boldsymbol{n}$ chosen as the polar axis of the coordinate system and $(\alpha, 0)$ denoting the angular coordinates of $\boldsymbol{h}$, one has $(\boldsymbol{e}\cdot\boldsymbol{h})^2 = (\cos\alpha\cos\theta + \sin\alpha\sin\theta\cos\phi)^2$. On taking the integrals over ϕ on the right-hand side of Eq. (3) and using the variable substitution $x = \cos(\theta)$ one gets

$$\langle(\boldsymbol{e}\cdot\boldsymbol{h})^2\rangle_0 = \frac{\int_0^1 \mathrm{d}x\,[\cos^2(\alpha)x^2 + \sin^2(\alpha)\tfrac{1}{2}(1-x^2)]\exp(\sigma x^2)}{\int_0^1 \mathrm{d}x \exp(\sigma x^2)}. \tag{4}$$

On using the function $R(\sigma) = \int_0^1 \mathrm{d}x \exp(\sigma x^2)$ and its σ-derivative $R'(\sigma) = \int_0^1 \mathrm{d}x\, x^2 \exp(\sigma x^2)$ [12], one can write the susceptibility as

$$\chi = \mu_0 \frac{M_s^2 V}{k_B T}\left[\cos^2(\alpha)\frac{R'}{R} + \sin^2(\alpha)\frac{R-R'}{2R}\right]. \tag{5}$$

In the following, when evaluating Eq. (5) for different choices of σ, the integrals defining $R(\sigma)$ and $R'(\sigma)$ are computed numerically using a method with an adaptive choice of the integration stepsize [13]. For large values of σ, the asymptotic expansions of R and R' are used [12]. On introducing the notations

$$\chi_\parallel = \mu_0 \frac{M_s^2 V}{k_B T}\frac{R'}{R}, \tag{6a}$$

$$\chi_\perp = \mu_0 \frac{M_s^2 V}{k_B T}\frac{R-R'}{2R}, \tag{6b}$$

the susceptibility reads $\chi = \cos^2(\alpha)\chi_\parallel + \sin^2(\alpha)\chi_\perp$. If this formula is averaged over a distribution of particle easy axes orientations, one finally gets for the susceptibility,

$$\chi = \langle\cos^2\alpha\rangle\chi_\parallel + \langle\sin^2\alpha\rangle\chi_\perp. \tag{7}$$

The assumption of a linear response allows for interpreting the first term in this formula as the average response to the field component along particle easy axis $H_\parallel = H\langle\cos\alpha\rangle$, and for interpreting the second term as the response to the field component perpendicular to that axis, $H_\perp = H\langle\sin\alpha\rangle$. In the low-temperature or, equivalently, large-barrier range, $\sigma \gg 1$, $\chi_\perp$ reaches the temperature independent value $\mu_0 M_s^2/2K$, whereas $\chi_\parallel \approx \chi_0 - \mu_0 M_s^2/K$, with $\chi_0 = \mu_0 M_s^2 V/k_B T$.

In a particle ensemble with a random orientation of the anisotropy axes, $\langle\cos^2\alpha\rangle = 1/3$ and $\langle\sin^2\alpha\rangle = 2/3$, hence, Eq. (7) is reduced to $\chi = \mu_0 M_s^2 V/3k_B T$, i.e., the Curie law for a superparamagnet is recovered. Thus, as previously mentioned, the equilibrium linear susceptibility of a monodispersed particle ensemble with randomly oriented easy axes is independent of the anisotropy constant K [2].

In a nonequilibrium situation, the magnetic relaxation induced by the field components $H_\parallel$ and $H_\perp$ are described by different relaxation times. In the case of the response to the field component being parallel to the anisotropy axis, the relaxation mechanism corresponds to a thermally activated inter-potential-well process and entails overcoming an energy barrier. In the large-barrier range, the characteristic time for this process is given by the Néel–Brown expression [1, 3]

$$\tau_\parallel = \tau_0 \exp(\sigma), \tag{8}$$

where τ_0 is a weakly temperature- and volume-dependent microscopic relaxation time related to intra-potential-well dynamics [14, 15], typically of the order 10^{-10} s. In the case of the field component being perpendicular to the anisotropy axis, the response corresponds to an intra-potential-well redistribution of the magnetic moments and its relaxation time, $\tau_\perp$, is of the order of τ_0 [6]. Thus, to account for the response of a magnetic particle system to a weak AC magnetic field, Shliomis and Stepanov [12] proposed a generalisation of Eq. (7) that consists of attaching Debye-like factors to each term in the equation for the susceptibility,

$$\chi = \langle\cos^2\alpha\rangle\chi_\parallel(1 + i\omega\tau_\parallel)^{-1} + \langle\sin^2\alpha\rangle\chi_\perp(1 + i\omega\tau_\perp)^{-1}. \quad (9)$$

Nevertheless, as $\tau_\perp \sim \tau_0$, particle magnetic moment responds *almost instantaneously* to $H_\perp$. More specifically, in AC susceptibility experiments, the condition $\omega\tau_\perp \ll 1$ will be fulfilled up to frequencies $\sim 10^7$ Hz. Very short measurement times, as, e.g., those obtained when performing inelastic neutron scattering [16] or ferromagnetic resonance experiments, are required in order to enable studies of the dynamics of the intra-potential-well response. Hence, on assuming $\omega\tau_\perp \ll 1$, and considering a random distribution of particle easy axes, Eq. (9) can be written as

$$\chi = \tfrac{1}{3}[\chi_\parallel(1 + i\omega\tau_\parallel)^{-1} + 2\chi_\perp]. \quad (10)$$

Eq. (10) was first proposed by Kumar and Dattagupta [17], who, considering both relaxation mechanisms, made an interesting analysis of the response of small magnetic particles to an AC field. Unfortunately, they considered $\chi_\parallel = \chi_0$ and $\chi_\perp = \mu_0 M_s^2/2K$, which do not fulfil the relation $\frac{1}{3}\chi_\parallel + \frac{2}{3}\chi_\perp = \mu_0 M_s^2 V/3k_B T$ and, hence, their χ does not have the correct static limit.

It is worth noting that the corresponding equation describing the behaviour of the time-dependent magnetisation, within the linear response regime, is given by

$$M(t)/H = \tfrac{2}{3}\chi_\perp + \tfrac{1}{3}\chi_\parallel[1 - \exp(-t/\tau_\parallel)]. \quad (11)$$

Owing to the $\omega\tau_\perp \ll 1$ assumption, this formula will be valid for observation times $t \gg \tau_\perp \sim \tau_0$. An equation equivalent to this was also proposed by Gittleman et al. [18], although they merely considered the approximations $\chi_\parallel \approx \chi_0 - \mu_0 M_s^2/K$ and $\chi_\perp \approx \mu_0 M_s^2/2K$.

If, instead of having a monodispersed particle system, the particle sizes are described by a normalised size distribution $g_V(V)$ [$g_V(V)\,dV$ is the volume fraction of particles with volumes between V and $V + dV$] and the anisotropy constant is the same for each particle, the in-phase and out-of-phase components of the AC susceptibility are given by

$$\chi' = \int_V \left\{\frac{1}{3}\chi_\parallel \frac{1}{1 + (\omega\tau_\parallel)^2} + \frac{2}{3}\chi_\perp\right\} g_V(V)\,dV, \quad (12a)$$

$$\chi'' = \int_V \frac{1}{3}\chi_\parallel \frac{\omega\tau_\parallel}{1 + (\omega\tau_\parallel)^2} g_V(V)\,dV, \quad (12b)$$

where it has been implicitly assumed that the particles within a given volume interval have their easy axes oriented at random. Alternatively, one can write this equation in terms of the distribution of energy barriers $g_E(E_b) = g_V(V)\,dV/dE_b = g_V(V)/K$, where $E_b = KV$. The integration of the corresponding expressions, presented in Section 4, will be truncated at $E_b = 4000$ K. This simplification will not introduce any significant error in the calculated results, since the only contribution to the susceptibility coming from particles (energy barriers) larger than that value will be their $\chi_\perp$ contribution, which will be in the order of $10^{-2}\chi_0$ or smaller. In addition, as will be discussed below, the particle size distribution for the sample used in the present study falls off exponentially at such large particle sizes.

3.2. The energy barrier (volume) distribution

In a recent publication [4] it was shown that the measured $\chi''(T)$ directly mirrors the distribution of energy barriers through the relation

$$g_E(E_b(\omega,T)) \approx \frac{2}{\pi}\frac{3K}{\mu_0 M_s^2}\frac{1}{E_b(\omega,T)}\chi''(\omega,T), \quad (13)$$

with $E_b(\omega,T) = -k_B T \ln(\omega\tau_0)$. This equation was derived assuming K to be sufficiently large so that $\chi_\parallel \approx \chi_0$ and $\chi_\perp \approx 0$. A more exact expression relating the out-of-phase component of the AC

susceptibility to the energy barrier distribution is given by

$$g_E(E_b(\omega,T)) \approx \frac{2}{\pi}\frac{3K}{\mu_0 M_s^2}\frac{1}{E_b(\omega,T)}\frac{R(\sigma_*)}{R'(\sigma_*)}\chi''(\omega,T), \quad (14)$$

where $\sigma_* \equiv E_b(\omega,T)/k_BT = -\ln(\omega\tau_0)$ is a temperature-independent parameter (thereby neglecting the weak temperature dependence of τ_0). Eq. (14) is a restatement of a similar equation appearing in Ref. [19] (although a factor $\pi/18$ appears to be missing in the equation derived in Ref. [19]). To derive Eq. (14), one uses the fact that the integrand in the equation for $\chi''(T)$ [Eq. (12b)] is peaked around $\tau_\parallel = 1/\omega$, implying that $\chi_\parallel(V)g_V(V)$ can be brought outside the integral with the volume set equal to $V_* = (k_BT/K)\sigma_* = -(k_BT/K)\ln(\omega\tau_0)$. The ratio $R(\sigma_*)/R'(\sigma_*)$ will thus (assuming a temperature independent τ_0) be independent of temperature. For typical AC field frequencies, $30\ \text{Hz} < \omega/2\pi < 3\times10^3$ Hz, the ratio $R(\sigma_*)/R'(\sigma_*)$ varies in the interval 1.06–1.10. Hence, using Eq. (14) will not alter the shape of the energy barrier distribution derived from Eq. (13), but merely change the value of the magnetic anisotropy constant thus derived.

Another method to derive the energy barrier distribution by means of the temperature derivative of $T\chi'$ [Ref. 5(a)] also exists. We will briefly show that this procedure, which goes back to Wohlfarth [20], could be less accurate than that of χ'' when the intra-potential-well contributions to the magnetic response play a significant role.

We start rewriting Eq. (12a) as

$$\chi' = \frac{\mu_0 M_s^2}{3k_BT}\int_0^\infty g_V(V)V\left\{1 - \frac{R'}{R}\frac{(\omega\tau_\parallel)^2}{1+(\omega\tau_\parallel)^2}\right\}dV \quad (15)$$

where Eqs. (6a) and (6b) has been used. On noting that the factor $(\omega\tau_\parallel)^2/[1+(\omega\tau_\parallel)^2] \approx 0$ for $V < V_*$ and $(\omega\tau_\parallel)^2/[1+(\omega\tau_\parallel)^2] \approx 1$ for $V > V_*$, one gets

$$\frac{\partial(T\chi')}{\partial T} \approx -\frac{\mu_0 M_s^2}{3k_B}\frac{\partial}{\partial T}\int_{V_*}^\infty g_V(V)V\frac{R'}{R}dV, \quad (16)$$

where the temperature dependence of M_s has been neglected [21]. The integral depends on T via the lower integration limit, V_*, and the argument of the functions R and R', $\sigma = KV/k_BT$. On taking the temperature derivative of the integral, one obtains

$$\frac{\partial(T\chi')}{\partial T} \approx \frac{\mu_0 M_s^2}{3K}\left\{g_V(V_*)V_*\frac{R'(\sigma_*)}{R(\sigma_*)}\sigma_* + \int_{V_*}^\infty g_V(V)\left[\frac{R''}{R} - \left(\frac{R'}{R}\right)^2\right]\sigma^2\,dV\right\} \quad (17)$$

where $R'' = dR'/d\sigma$. This equation generalises that of Slade et al. [Ref. 5(a)], which would be obtained if one started the derivation with $\chi_\parallel \approx \chi_0$ and $\chi_\perp \approx 0$. It is thus shown that when a nonzero $\chi_\perp$ is accounted for, the presence of the second term on the right-hand side of Eq. (17), which contains information about $g_V(V)$ in integral form, implies that $\partial(T\chi')/\partial T$ does not mirror the particle volume distribution in the same direct way as χ'' does.

This fact can conveniently be restated considering how the relation

$$\chi'' = -\frac{\pi}{2}\frac{1}{\ln(\omega\tau_0)}\frac{\partial(T\chi')}{\partial T},$$

derived in Ref. [22], is modified when $\chi_\perp \neq 0$ is considered. On rewriting Eq. (14) in terms of $g_V(V)$, using this expression to eliminate $g_V(V)$ from the first term on the right-hand side of Eq. (17), and solving for χ'', one gets

$$\chi'' \approx -\frac{\pi}{2}\frac{1}{\ln(\omega\tau_0)}\left\{\frac{\partial(T\chi')}{\partial T} - \frac{\mu_0 M_s^2}{3K}\int_{V_*}^\infty g_V(V)\left[\frac{R''}{R} - \left(\frac{R'}{R}\right)^2\right]\sigma^2\,dV\right\}. \quad (18)$$

Since σ runs from $\sigma_* = -\ln(\omega\tau_0) \sim 20$–$30$ to infinity within the integral, one can use the asymptotic formulae for R and its derivatives [12] to obtain $[R''/R - (R'/R)^2] \approx 1/\sigma^2 + \cdots$, which introduced into Eq. (18) yields

$$\chi'' \approx -\frac{\pi}{2}\frac{1}{\ln(\omega\tau_0)}\left\{\frac{\partial(T\chi')}{\partial T} - \frac{\mu_0 M_s^2}{3K}\int_{V_*}^\infty g_V(V)\,dV\right\}. \quad (19)$$

The aforementioned relation of Lundgren et al. [22] is recovered in the limit $K\to\infty$ or, equivalently, if one derives Eq. (18) considering $\chi_\parallel \approx \chi_0$ and $\chi_\perp \approx 0$ from the beginning. Eqs. (18) and (19)

are generalisations of such a relation when the intra-potential-well response is taken into account. The second term within the curly brackets of Eq. (19) corresponds to minus the contribution of blocked ($V > V_*$) particles to the AC susceptibility at $T = 0$. Even for this special case, $\partial(T\chi')/\partial T$ does not scan the energy barrier distribution as exactly as χ'' does.

Eqs. (17)–(19) indicate that the determination of the barrier (volume) distribution by means of $\partial(T\chi')/\partial T$ will be correct only in those cases when the intra-potential-well contributions to the susceptibility can be neglected. On the other hand, the determination of the barrier (volume) distribution using χ'' [Eq. (14)] *is not restricted* by such a condition.

Tests of Eq. (19) and the relation derived in Ref. [22] are probably best performed using results obtained from measurements on noninteracting magnetic particle systems. Admittedly, the relation derived by Lundgren et al. was initially used in connection with experiments on spin glasses. However, spin glasses are intimately connected with magnetic interactions and collective dynamics, effects which are not explicitly treated in the derivation of this relation.

4. Results

In a recent publication [4], Eq. (13) was used to extract the energy barrier distribution for the same ferrofluid sample as used in the present work. The distribution was determined in the energy interval $100\ \mathrm{K} < E_b < 1500\ \mathrm{K}$. The extracted distribution $g_E(E_b)$ compares remarkably well with a normalised Gamma distribution

$$g_E(E_b) = \frac{b^{-1}}{\Gamma(1+a)}\left(\frac{E_b}{b}\right)^a \exp(-E_b/b) \qquad (20)$$

where $\Gamma(\cdot)$ is the gamma function. The parameters of the distribution function were determined as $a = 0.5585$ and $b = 168.7\ \mathrm{K}$. Moreover, it was shown that this distribution can be used to calculate $\chi''(T)$-curves that compare to a high degree of precision with the corresponding experimental results. The calculations in Ref. [4] were performed assuming $\chi_\parallel \approx \chi_0$ and $\chi_\perp \approx 0$, thereby neglecting intra-potential-well contributions to the magnetic response. The importance of this contribution is however best seen when comparing calculated $\chi'(T)$-curves with the corresponding experimental ones. In Fig. 1, calculated $\chi'(T)$- and $\chi''(T)$-curves, assuming $\chi_\parallel \approx \chi_0$ and $\chi_\perp \approx 0$, are visualised together with the corresponding experimental results. The calculations were performed using $K = 14.7\ \mathrm{kJ/m^3}$ and $\tau_0 = 4 \times 10^{-10}\ \mathrm{s}$ [4]. While the calculated and experimental $\chi''(T)$-curves compare to a high degree of precision, the resemblance between the calculated and experimental $\chi'(T)$-curves is rather poor. It is worth pointing out that the calculated and experimental $\chi'(T)$-curves differ not only in magnitude but also in shape.

In order to explain the discrepancy between the calculated and experimental $\chi'(T)$-curves, it is important to account for the intra-potential-well contribution to the susceptibility. This contribution is included by calculating $\chi_\parallel$ and $\chi_\perp$ according to Eqs. (6a) and (6b). Inspection of Eqs. (13) and (14), accounting for the almost constant value of $R(\sigma_*)/R'(\sigma_*)$, indicates that when computing the $\chi''(T)$-curves one should not expect a significant influence of the use of Eq. (6a) to define $\chi_\parallel$, instead of using the more simple $\chi_\parallel = \chi_0$. This can be viewed as follows. The perpendicular component of the susceptibility does not include dispersion. Hence, the only difference is the presence of a factor R'/R in the integrand of Eq. (12b), as compared with the corresponding equation of the $\chi_\parallel = \chi_0$ model, which, as argued above, can be brought outside the integral. Thus, the only noticeable effect is the occurrence of the approximately temperature independent ratio $R(\sigma_*)/R'(\sigma_*)$ in the expression for the out-of-phase component of the AC susceptibility. This merely implies, assuming that we know the saturation magnetisation of the magnetic particle system, that the magnetic anisotropy constant needs to be re-normalised by the same factor in order for the calculated $\chi''(T)$ results to compare in magnitude with the corresponding experimental results.

In Fig. 2, calculated $\chi'(T)$- and $\chi''(T)$-curves, using Eqs. (6a) and (6b) to calculate $\chi_\parallel$ and $\chi_\perp$ needed in Eqs. (12a) and (12b), are visualised together with the experimental AC susceptibility results. The

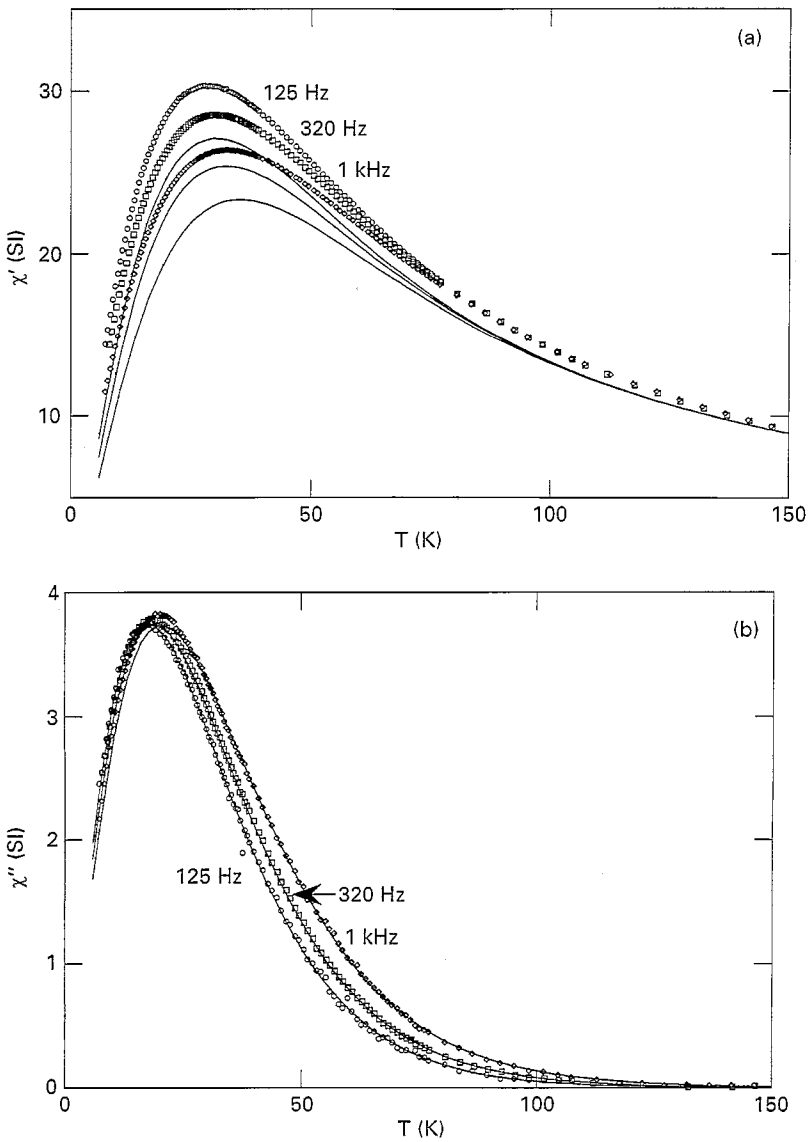

Fig. 1. Calculated (solid lines) and experimental (open symbols) ac susceptibility curves. The different curves correspond to different frequencies f. The calculations were performed using $\chi_{\parallel}(V) = \chi_0(V)$ and $\chi_{\perp}(V) = 0$. $K = 14.7$ kJ/m^3 and $\tau_0 = 4 \times 10^{-10}$ s. (a) $\chi'(T)$ and (b) $\chi''(T)$.

calculations were performed using $K = 13.4$ kJ/m^3 and $\tau_0 = 4 \times 10^{-10}$ s. Including both inter-potential- and intra-potential-well contributions to the magnetic response, the similarity between calculated and experimental $\chi'(T)$-curves improves considerably. Clearly, this indicates that the intra-potential-well contribution has to be included in order to give a full description of the dynamic susceptibility. It is also worth pointing out that the $\sigma \gg 1$ approximations of Eqs. (6a) and (6b), i.e. $\chi_{\parallel} \approx \chi_0 - \mu_0 M_s^2/K$ and $\chi_{\perp} \approx \mu_0 M_s^2/2K$, result in calculated curves showing a similarly good agreement with the experimental curves. However, the approach of Kumar and Dattagupta [17], i.e.,

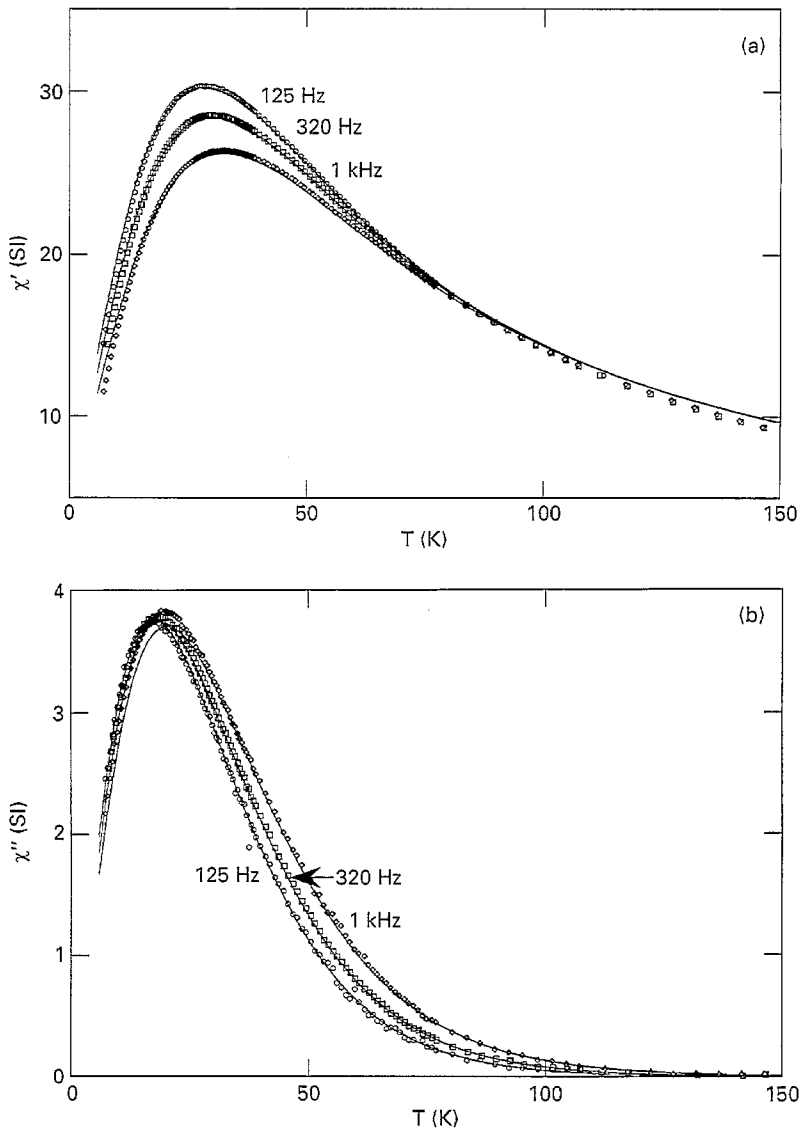

Fig. 2. Calculated (solid lines) and experimental (open symbols) AC susceptibility curves. The different curves correspond to different frequencies f. The calculations were performed using Eqs. (6a) and (6b) to calculate $\chi_{\parallel}(V)$ and $\chi_{\perp}(V)$. $K = 13.4\ \mathrm{kJ/m^3}$ and $\tau_0 = 4 \times 10^{-10}$ s. (a) $\chi'(T)$ and (b) $\chi''(T)$.

using $\chi_{\parallel} \approx \chi_0$ and $\chi_{\perp} \approx \mu_0 M_s^2/2K$, will not give a consistent description of the AC susceptibility, since in this case one obtains $\chi'(T)$-curves larger than the corresponding experimental curves.

When closely examining Fig. 2, it is possible to discern small discrepancies between the calculated and experimental $\chi'(T)$-curves at high ($T > 100$ K) and low temperatures ($T < 15$ K). A possible cause for the observed difference at low temperatures is that the used energy barrier distribution overestimates the statistical weight in the low-energy tail of the distribution (the experimentally determined distribution only covered energy barriers larger than 100 K). The difference at high temperatures can

tentatively be explained by the temperature dependence of the saturation magnetisation of the magnetic particle system, which has so far been neglected.

In Fig. 3, a comparison between calculated, accounting for a temperature-dependent M_s and that the used Gamma distribution possibly overestimates the statistical weight in the low-energy tail of

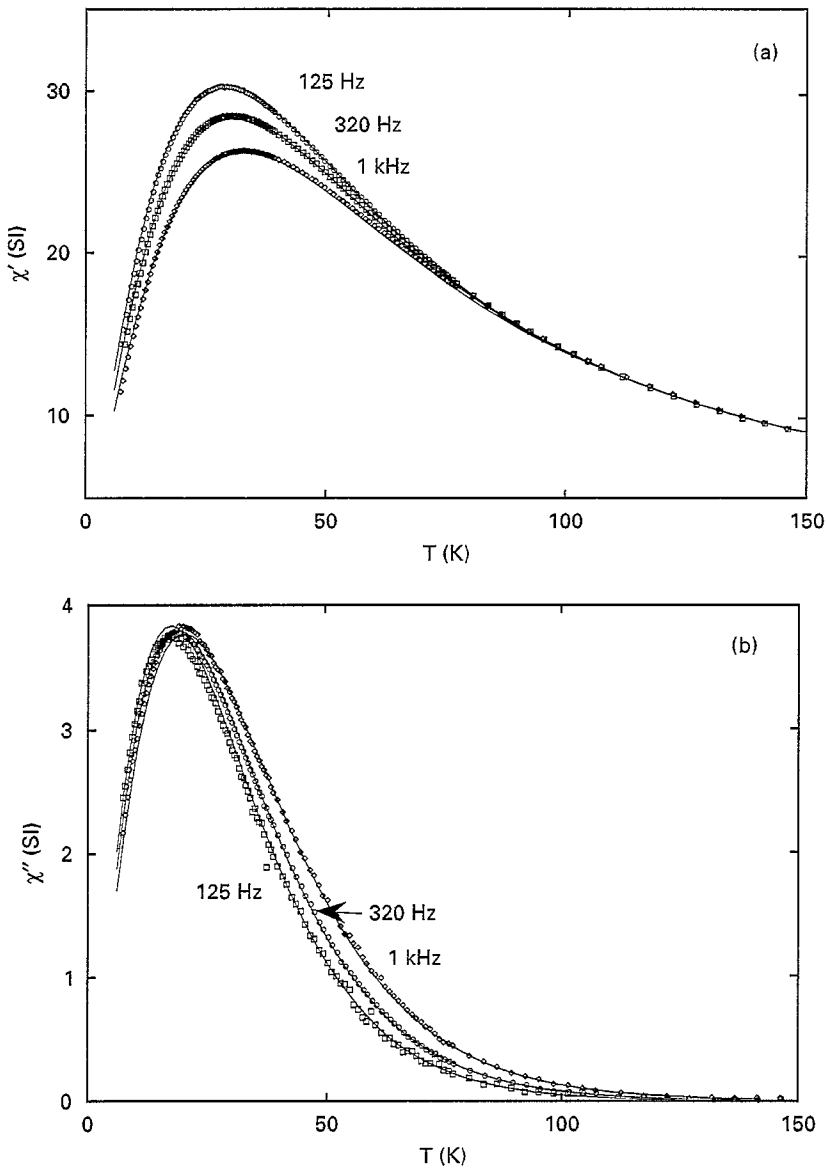

Fig. 3. Calculated (solid lines) and experimental (open symbols) AC susceptibility curves. The different curves correspond to different frequencies f. The calculations were performed using Eqs. (6a) and (6b) to calculate $\chi_{\parallel}(V)$ and $\chi_{\perp}(V)$. In addition, a temperature dependence of the saturation magnetisation was used as well as a cut-off in the Gamma energy barrier distribution at $E_b = 38$ K (the statistical weight for energy barriers smaller than this energy was set to zero). $K = 13.2$ kJ/m^3 and $\tau_0 = 4 \times 10^{-10}$ s. (a) $\chi'(T)$ and (b) $\chi''(T)$.

the distribution, and experimental AC susceptibility curves are visualised. The temperature dependence of the saturation magnetisation was modelled as $\Delta M_s/M_s(0) = 1.8 \times 10^{-5} T^{3/2}$, which is of a similar magnitude as what has been measured for a concentrated maghemite sample (the concentration by volume of particles in this sample was $\sim 17\%$) taken from the same batch of ferrofluid [23]. To correct for a possible overestimate of the weight in the low-energy tail of the energy barrier distribution, a cut-off in the Gamma distribution was introduced at $E_b = 38$ K (the weight for energy barriers lower than this value was set to zero). As can be seen in Fig. 3, the proposed modifications of the model eliminate most of the differences observed between calculated and experimental results in Fig. 2. It should be pointed out, however, that other simplifications used in the theoretical modelling, such as neglecting the temperature and volume dependence of the microscopic relaxation time τ_0, may also contribute to the observed differences.

Eqs. (17)–(19) suggest the plotting of χ'' and $-[(\pi/2)/\ln(\omega\tau_0)]\partial(T\chi')/\partial T$ versus $-T\ln(\omega\tau_0)$ as an alternative way of showing the necessity of including an intra-well response in the theoretical modelling of the AC susceptibility. In the case of the intra-potential-well contribution to the magnetic response being negligible, these two curves should trace out the same energy barrier dependence and thus determine the same energy barrier distribution. This is what one observes when performing this analysis using the theoretical curves shown in Fig. 1. If, however, the intra-potential-well contribution to the magnetic response cannot be neglected, one would, according to Eqs. (18) and (19), expect $-[(\pi/2)/\ln(\omega\tau_0)]\,\partial(T\chi')/\partial T$ to be larger than χ''. Moreover, the difference between the two curves is expected to be larger at lower temperatures, since when decreasing the temperature the lower integration limit in Eqs. (18) and (19) decreases. This is what is observed in Fig. 4, where χ'' and $-[(\pi/2)/\ln(\omega\tau_0)]\partial(T\chi')/\partial T$ are plotted versus energy barrier $E_b(\omega,T)/k_B = -T\ln(\omega\tau_0)$. This plot gives further evidence for the necessity of including an intra-potential-well contribution to the magnetic response of this nano-sized magnetic particle system. The figure also confirms the notion that

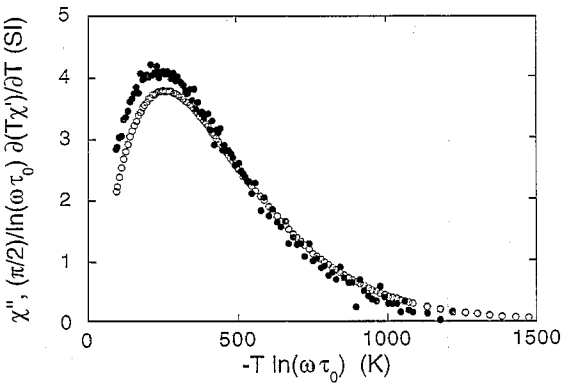

Fig. 4. χ'' (open symbols) and $-[(\pi/2)/\ln(\omega\tau_0)]\partial(T\chi')/\partial T$ (filled symbols) versus $E_b(\omega,T)/k_B = -T\ln(\omega\tau_0)$. $\omega/2\pi = 320$ Hz and $\tau_0 = 4 \times 10^{-10}$ s.

$-[(\pi/2)/\ln(\omega\tau_0)]\,\partial(T\chi')/\partial T$ does not determine the energy barrier distribution as accurately as χ'' does.

An alternative way of showing the influence of intra-potential-well fluctuations is to study the behaviour of the phase $\varphi = \tan^{-1}(\chi''/\chi')$. The significance of such fluctuations has neatly been pointed out in a theoretical study of a 1D bistable system driven by an oscillating field [24]. It was shown that, unlike in a model disregarding intra-potential-well fluctuations, the phase when plotted versus temperature exhibits a maximum when intra-potential-well fluctuations are considered. This maximum of the phase is interpreted as being due to competition between intra-potential- and inter-potential-well motions and hence depends on the very existence of the former [25]. Fig. 5 shows the phase behaviour of the theoretical models used in Figs. 1 and 3, along with that of the experimental results. Whereas the experimental data and the model which takes intra-potential-well fluctuations into account show the expected maxima of φ, the model with $\chi_\parallel \approx \chi_0$ and $\chi_\perp \approx 0$ shows a monotonic increase of φ with decreasing temperature. As the phase behaviour is an intrinsic characteristic of each model, Fig. 5 illustrates that the discrepancies between the experimental results and the model which excludes intra-well fluctuations are not merely quantitative but also qualitative.

The discrepancy between the experimental φ-curves and the corresponding calculated curve, including intra-potential-well fluctuations, near the

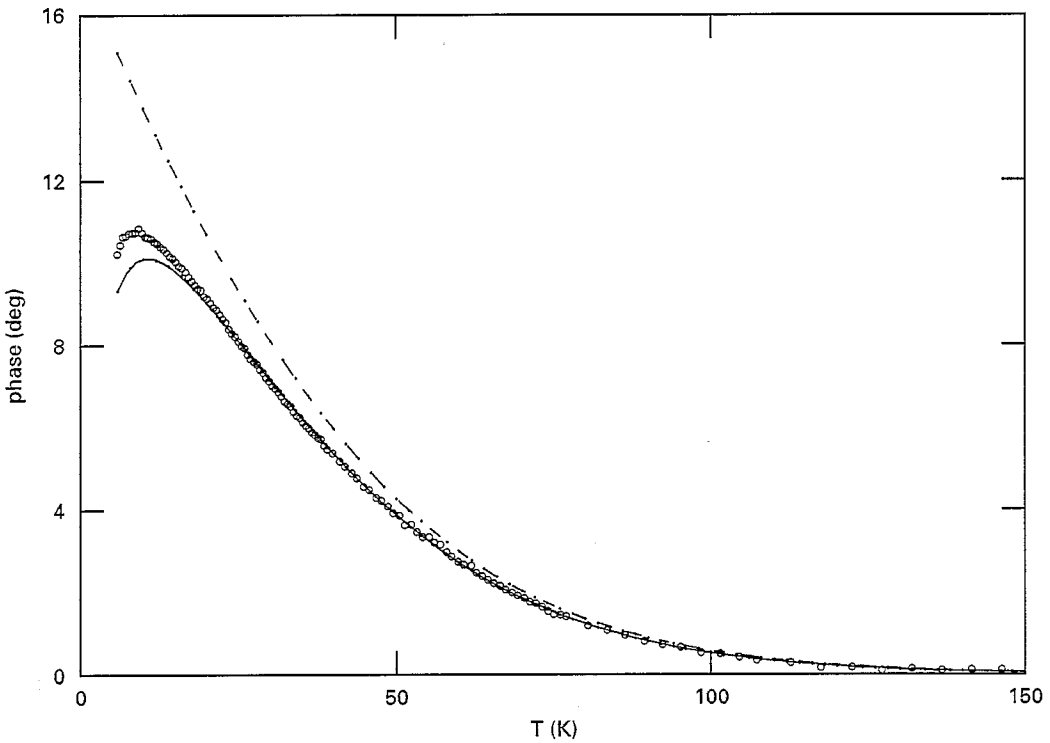

Fig. 5. $\varphi = \tan^{-1}(\chi''/\chi')$ versus temperature. The solid and dashed lines were obtained using the theoretical models with and without intra-potential-well fluctuations, respectively, while the experimental results are shown by open symbols. $\omega/2\pi = 1$ kHz.

maxima in the φ-curves, is explained by the aforementioned uncertainty in the determination of the energy barrier distribution at low energy barrier values (<100 K). This indicates that the low-temperature behaviour of φ can be used to more accurately assess the energy barrier distribution at low energy barriers. This may prove to be very helpful when trying to distinguish between magnetic relaxation governed by thermally activated dynamics and quantum tunnelling of the particle magnetic moments [25]. A particular shape of the energy barrier distribution in the low energy limit can if the exact form of the distribution is unknown, result in a magnetic response that is erroneously attributed to quantum tunnelling of the particle magnetic moments.

Finally, it is worth noting that the approximation $\chi_{\|} \approx \chi_0$ and $\chi_{\perp} \approx 0$, together with Eqs. (12a) and (12b), could be interpreted as a model where one fully takes into account the intra-potential-well response, via its effects on the equilibrium response, and then assumes one relaxation mechanism for the overall response [cf. Eq. (11)],

$$M(t)/H = \tfrac{1}{3}(\chi_{\|} + 2\chi_{\perp})\,[1 - \exp(t/\tau_{\|})] = \tfrac{1}{3}\chi_0[1 - \exp(t/\tau_{\|})] \quad (21)$$

where $\chi_{\|}$ and $\chi_{\perp}$ are calculated according to Eqs. (6a) and (6b). Apart from its dubious foundation, the proven failure of the $\chi_{\|} \approx \chi_0$ and $\chi_{\perp} \approx 0$ approximation to reproduce the experimental results points to the inadequacy of this model, and hence to the necessity of including different relaxation times for each response.

5. Conclusions

Raikher and Stepanov have theoretically proved that intra-well motions are essential, especially at

low temperatures, for obtaining a correct description of the dynamics of the particular case of single-domain magnetic particles whose easy axes are aligned along the applied field [26].

In this paper, to be able to reproduce the measured in-phase and out-of-phase components of the AC susceptibility in a particle ensemble whose easy axes are randomly distributed, it was necessary to include intra-potential- as well as inter-potential-well contributions to the magnetic response. Moreover, it has been shown that different relaxation times need to be assigned to the two contributions. In other works, the $\chi_\perp$ contribution has either been left out completely [4, 5], or the approximation $\chi_\perp \approx \mu_0 M_s^2/2K$ has been used, either considering $\chi_\parallel \approx \chi_0$ [17, 27] (i.e. inconsistently neglecting intra-potential-well thermal fluctuations), or more correctly $\chi_\parallel \approx \chi_0 - \mu_0 M_s^2/K$ [18]. The present work indicates that not only is it necessary to include a $\chi_\perp$ contribution, but one also has to allow for fluctuations inside the potential-wells. Consequences, when including a $\chi_\perp$ contribution to the magnetic response, for methods using AC susceptibility results to determine the distribution of energy barriers (particle volumes) have also been pointed out.

Acknowledgements

Financial support from the Swedish Natural Science Research Council (NFR) is gratefully acknowledged. One of us, J.L.G.-P., thank DGA for a grant (BIT 1292, CONSI + D).

References

[1] L. Néel, Ann. Géophys. 5 (1949) 99.
[2] C.J. Lin, J. Appl Phys. 32 (1961) 233s; V.V. Shcherbakova, Izv. Earth Phys. 14 (1978) 308; R.W. Chantrell, N.Y. Ayoub and J. Popplewell, J. Magn. Magn. Mater. 53 (1985) 199.
[3] W.F. Brown, Jr., Phys. Rev. 130 (1963) 1677.
[4] T. Jonsson, J. Mattsson, P. Nordblad and P. Svedlindh, J. Magn. Magn. Mater. 168 (1997) in print.
[5] (a) S.B. Slade, L. Gunther, F.T. Parker and A.E. Berkowitz, J. Magn. Magn. Mater. 140–144 (1995) 661; (b) F.J. Lázaro, J.L. García, V. Schünemann, Ch. Butzlaff, A. Larrea and M.A. Zaluska-Kotur, Phys. Rev. B 53 (1996) 13934.
[6] A. Labarta, O. Iglesias, Ll. Balcells and F. Badia, Phys. Rev. B 48 (1993) 10240.
[7] E. Vincent, J. Hammann, P. Prené and E. Tronc, J. Phys. I France 4 (1994) 273.
[8] O. Iglesias, F. Badia, A. Labarta and Ll. Balcells, J. Magn. Magn. Mater. 140–144 (1995) 399.
[9] Ferrofluids Co., Nashua, New Hampshire.
[10] Ferromagnetic Materials, Vol. 2, ed. E.P. Wohlfahrth (North-Holland, Amsterdam, 1980).
[11] T. Jonsson, J. Mattsson, C. Djurberg, F.A. Khan, P. Nordblad and P. Svedlindh, Phys. Rev. Lett. 75 (1995) 4138.
[12] M.I. Shliomis and V.I. Stepanov, J. Magn. Magn. Mater. 122 (1993) 176.
[13] Numerical Recipes in Fortran (Cambridge University Press, New York, 1992).
[14] W.F. Brown, Jr., Phys. Rev. 130 (1969) 1677.
[15] W.T. Coffey, D.S.F. Crothers, Yu.P. Kalmykov, E.S. Massawe, Phys. Rev. E 49 (1994) 1869; W.T. Coffey, D.S.F. Crothers, Yu.P. Kalmykov, E.S. Massawe and J.T. Waldron, J. Magn. Magn. Mater. 127 (1993) L254; W.T. Coffey, P.J. Cregg, D.S.F. Crothers, J.T. Waldron and A.W. Wickstead, J. Magn. Magn. Mater. 131 (1994) L301.
[16] M. Hennion et al., Europhys. Lett. 25 (1994) 43.
[17] D. Kumar and S. Dattagupta, J. Phys. C 16 (1983) 3779.
[18] Gittleman, B. Abeles and S. Bozowski, Phys. Rev. B 9 (1974) 3891.
[19] M.I. Shliomis and V.I. Stepanov, Adv. Chem. Phys. 87 (1994) 1.
[20] E.P. Wohlfarth, Phys. Lett. A 70 (1979) 489 and J. Phys. F 10 (1980) L241.
[21] If $M_s(T)$ has to be accounted for, the analysis can readily be performed considering $\partial(T\chi' M_s^{-2})/\partial T$ instead of $\partial(T\chi')/\partial T$.
[22] L. Lundgren, P. Svedlindh and O. Beckman, J. Magn. Magn. Mater. 25 (1981) 33.
[23] Unpublished, $\Delta M_s/M_s(0) = 3.4 \times 10^{-5} \times T^{3/2}$ for the concentrated sample.
[24] M. Morillo and J. Gómez-Ordóñez, Phys. Rev. Lett. 71 (1993) 9.
[25] B. Barbara et al., in: Magnetic Properties of Fine Particles, Eds. J.L. Dormann and D. Fiorani (North-Holland, Amsterdam, 1992) p. 235.
[26] Yu.L. Raikher and V.I. Stepanov, Phys. Rev. B 52 (1995) 3493.
[27] F.J. Lázaro, J.L. García, F. Schünemann and A.X. Trautwein IEEE Trans. Mag. 29 (1993) 2652; B. Barbara et al., in: Magnetic Properties of Fine Particles, Ed. J.L. Dormann and D. Fiorani (North-Holland, Amsterdam, 1992) p. 235.